



Restoration of solid oxide fuel cell stacks after failure of partial cells

M. Yokoo*, Y. Tabata, Y. Yoshida, K. Hayashi, Y. Nozaki, K. Nozawa, H. Arai

NTT Energy and Environment Systems Laboratories, NTT Corporation, 3-1 Morinosato Wakamiya, Atsugi-shi, Kanagawa 243-0198, Japan

ARTICLE INFO

Article history:

Received 27 November 2008
Received in revised form 5 January 2009
Accepted 15 January 2009
Available online 21 January 2009

Keywords:

Solid oxide fuel cell
Cell stack
Restoration after cells failure

ABSTRACT

We investigated a solid oxide fuel cell stack that employs anode-supported planar cells in which two intermediate plates are installed every 10 cells to determine the influence of the separation and reconnection of the intermediate plates after high temperature operation. We showed that this separation and reconnection caused no significant degradation in stack performance. A 30-cell stack, which was constructed by removing two 10-cell sub-stacks from a 50-cell stack that had operated stably 1200 h, functioned well. The difference between the average voltages of the cells in the 50- and 30-cell stacks was less than 3% when the current density, fuel utilization, and oxygen utilization were 0.30 A cm^{-2} , 60%, and 15%, respectively. The 30-cell stack operated stably for about 1200 h with almost no degradation. These findings indicate that our stack can be restored after cells in the stack have broken down simply by removing the 10-cell sub-stacks that contain the broken cells and replacing them with undamaged 10-cell sub-stacks.

© 2009 Elsevier B.V. All rights reserved.

1. Introduction

Solid oxide fuel cells (SOFC) have been attracting attention because of their high electrical conversion efficiency, which exceeds 50% [1–3]. We have been developing a power generation system that employs an SOFC for use in our communication bases, where electricity is more important than heat as an energy source. The key to establishing a highly efficient fuel cell system is the performance of the fuel cells and cell stacks.

We have already developed an SOFC with an anode-supported structure that provides a high power density [4,5]. The anode-supported structure allows the use of a thin electrolyte, which provides a low electrical resistance. We use scandia-alumina stabilized zirconia (SASZ) as the electrolyte, because of its high ionic conductivity [4,5]. A cermet consisting of nickel oxide and SASZ is used for the anode, which has a double-layer structure [5]. Furthermore, as the cathode material we use lanthanum nickel ferrite (LNF), which has a high electrical conductivity and is resistant to chromium poisoning [6–9].

We have also developed a highly efficient and durable SOFC stack with an internal manifold structure by using our anode-supported cells [10–12]. A stack using 25 cells (100-mm-diameter) provided an output of 350 W and an electrical conversion efficiency of 56% based on the lower heating value (LHV) of methane, which was used as a fuel [10,11]. The output and efficiency were maintained for over 1100 h [10,11]. Furthermore, a 50-cell stack using 120-mm-diameter

cells provided an output of 1100 W [12]. The energy conversion efficiency and durability of the 50-cell stack were almost the same as those of the 25-cell stack [12].

Our SOFC stacks provided acceptable efficiency and durability. However, these stacks, in which all the cells are electrically connected in series, are difficult to be restored when one cell in the stack breaks down. This is because it is difficult to replace only the broken part since the metal plates used as the stack components bonded together after high temperature operation. It is desirable to restore the stacks simply by replacing the broken part.

This paper presents the results of a basic investigation into restoring the stacks solely by replacing the broken part. In particular, we describe the influence on stack performance of the disassembly and reassembly of the stack after high temperature operation.

2. Stack configuration

Our stacks were constructed by combining power generation units, each of which had 1 anode-supported cell and 5 metal plates as its main components [11,12]. The 1.0-mm-thick metal plates were made of corrosion resistant ferritic stainless steel.

When we constructed the stacks, we occasionally introduced intermediate plates that were 2.5-mm-thick [12]. Two intermediate plates were inserted in the stacks every 10 power generation units as shown in Fig. 1. Here, Fig. 1 shows a 50-cell stack with intermediate plates. When we disassembled the stacks containing intermediate plates after high temperature operation, we separated the intermediate plates as shown in Fig. 2. We refer to a set of 10 power generation units as a 10-cell sub-stack. By contrast, stacks

* Corresponding author. Tel.: +81 46 240 2572; fax: +81 46 270 2702.
E-mail address: m.yokoo@aecl.ntt.co.jp (M. Yokoo).

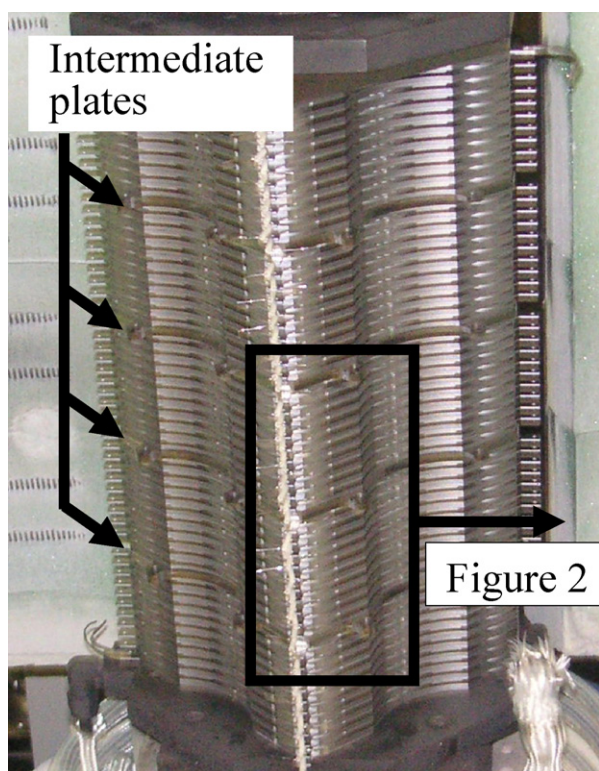


Fig. 1. 50-cell stack with intermediate plates.

without intermediate plates were disassembled by separating the power generation units from each other after high temperature operation as shown in Fig. 3.

3. Experiments

3.1. Stack without intermediate plates

A 50-cell stack without intermediate plates was constructed by using cells that were 100 mm in diameter. The 100-mm-diameter

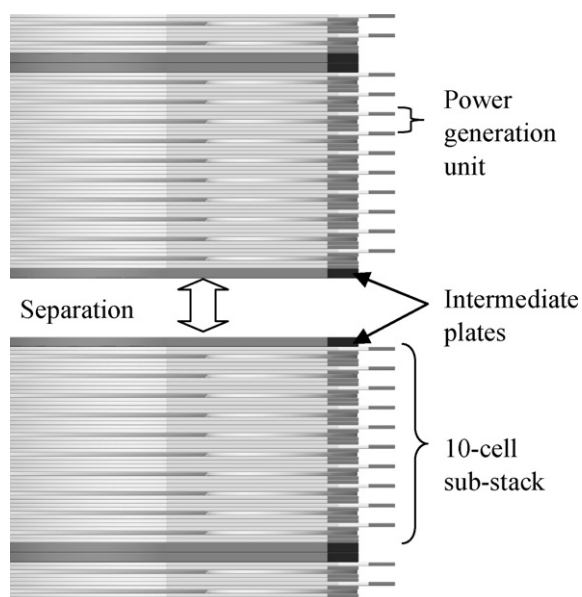


Fig. 2. Separation of intermediate plates.

cell has an active electrode area of 60 cm^2 . The configuration of the system we used for evaluating the 50-cell stack has been previously reported [11,12]. Dry hydrogen was used as a fuel and dry air was used as an oxidant. The 50-cell stack was installed in an electric furnace with three zones. The temperature of the three zones was set at 1073 K.

The voltages of stack and power generation units were measured as a function of current density after the anodes of the cells had been reduced by hydrogen. Surface temperature was measured for power generation units 10, 20, 30, and 40 with thermocouples. The power generation units were numbered from the bottom in this paper. AC impedance measurement was carried out for all the power generation units under an open circuit condition. After measuring the voltages as a function of current density, we operated the stack at a current density of 0.3 A cm^{-2} .

The 50-cell stack was disassembled by separating the power generation units after the power generation test.

3.2. Stack with intermediate plates

Cells with a diameter of 100 mm were also used in a 50-cell stack with intermediate plates. The evaluation system and experimental procedure for the power generation test on the 50-cell stack with intermediate plates were the same as those used for the 50-cell stack without intermediate plates.

After the power generation test, the 50-cell stack was divided into five 10-cell sub-stacks by separating the intermediate plates. Then, we reassembled a 30-cell stack with intermediate plates using three 10-cell sub-stacks. Fig. 4 shows the configuration of the 30-cell stack in detail. Here, the 10-cell sub-stacks A, B, C, D, and E were composed of power generation units 1–10, 11–20, 21–30, 31–40, and 41–50, respectively. As shown in Fig. 4, the 10-cell sub-stacks B and D were removed from the 50-cell stack, and the 30-cell stack was composed of the 10-cell sub-stacks A, C, and E. For the 30-cell stack, we measured the voltage drop between the 10-cell sub-stacks as shown in Fig. 4.

The evaluation system for the 30-cell stack with intermediate plates was the same as that used for the 50-cell stacks with and without intermediate plates. Surface temperature was measured for power generation units 10, 30, and 50 with thermocouples. AC impedance measurement was carried out for all the power generation units under an open circuit condition. We measured voltages of stack and power generation units as a function of current density, and then operated the stack at a current density of 0.3 A cm^{-2} .

4. Results and discussion

4.1. Stack without intermediate plates

The surface temperatures of the power generation units were $1078 \pm 5 \text{ K}$ under an open circuit condition in a 50-cell stack without intermediate plates. There were little differences in the AC impedance spectra under the open circuit condition among all the power generation units. The direct current resistances, which are intersection points of real part axis in Cole–Cole plot of AC impedance spectra, were about $0.5 \Omega \text{ cm}^2$ for all the power generation units. The relationship between average unit voltage and current density was almost the same with the relationship between voltage and current density in a single 100-mm-diameter cell. Here, the average unit voltage was calculated by dividing the total stack voltage by the number of power generation units. The initial performance of the 50-cell stack was acceptable. The surface temperatures of the power generation units were $1083 \pm 5 \text{ K}$ at a current density of 0.3 A cm^{-2} . Though the temperatures at the current density of 0.3 A cm^{-2} were slightly higher than those under the open

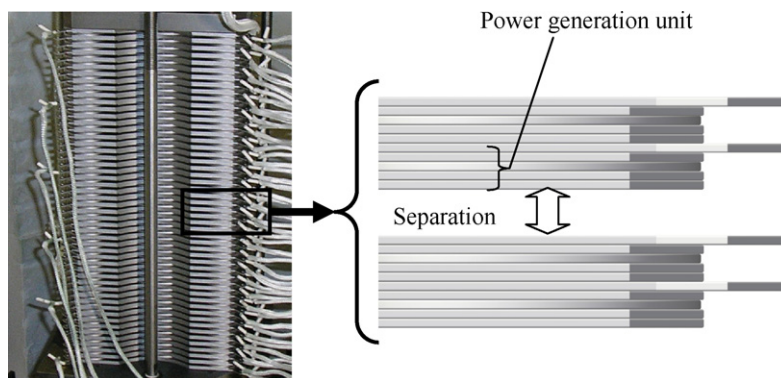


Fig. 3. Separation of power generation units.

circuit condition, there was little change in the temperature gradient. The fluctuation in the voltages of the power generation units was $\pm 5\%$ at the current density of 0.3 A cm^{-2} . This agrees with the results that the AC impedance spectra under the open circuit condition were almost the same for all the power generation units and that the temperature gradient in the stack was still small at the current density of 0.3 A cm^{-2} . Moreover, these results suggest that the hydrogen and air was distributed to all the power generation units almost equally.

Then, we operated the stack at a current density of 0.3 A cm^{-2} and at a fuel utilization of 60%. However, the average unit voltage for the 50-cell stack fell immediately. This is because one cell in the 50-cell stack broke down. We believe that this occurred because errors related to the position and angle of the stack parts were so large that the stack parts were not arranged properly [12]. We had planned to operate the stack at a fuel utilization of 70%, but the cell in the stack broke down before we increased the fuel utilization from 60% to 70%.

After the power generation test, we separated the power generation unit with the broken cell and tried to replace it with an undamaged power generation unit. However, the metal plates of

the power generation units were severely deformed by the separation process, and it was impossible to reconnect the surfaces of the separated units.

4.2. Stack with intermediate plates

As with the stack without intermediate plates, the surface temperatures of the power generation units were $1078 \pm 5 \text{ K}$ and the AC impedance spectra were almost the same for all the power generation units under an open circuit condition in a 50-cell stack with intermediate plates. The direct current resistances were about $0.5 \Omega \text{ cm}^2$ for all the power generation units. The initial characteristic of the 50-cell stack was almost the same as that of a single cell. The surface temperatures of the power generation units were $1083 \pm 5 \text{ K}$ and the fluctuation in the voltages of the power generation units was $\pm 5\%$ at a current density of 0.3 A cm^{-2} . Furthermore, the 50-cell stack operated stably for about 1200 h as shown in Fig. 5. During this long-term operation, the current density, fuel utilization, and oxygen utilization were kept at 0.3 A cm^{-2} , 70%, and 15%, respectively. The durability of the 50-cell stack was acceptable. The intermediate plates were effective as regards cancelling out cumu-

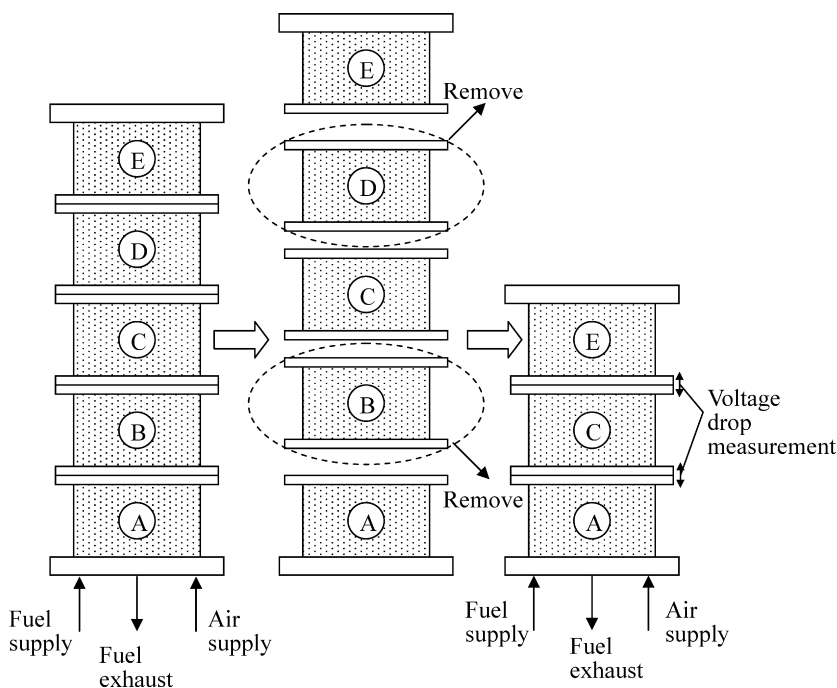


Fig. 4. Configuration of 30-cell stack (sub-stack A: power generation units 1–10, sub-stack B: power generation units 11–20, sub-stack C: power generation units 21–30, sub-stack D: power generation units 31–40, sub-stack E: power generation units 41–50).

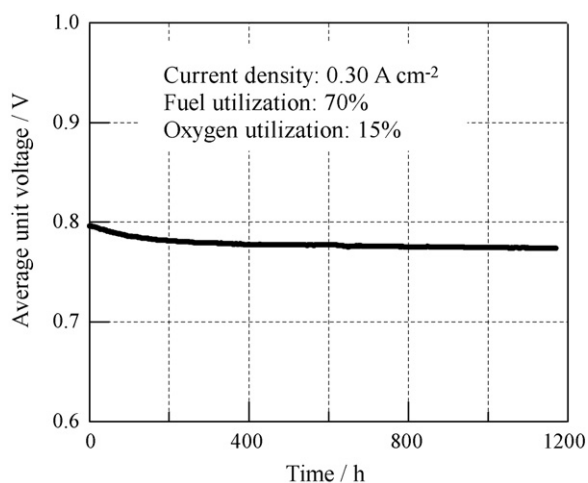


Fig. 5. Temporal change in average unit voltage for 50-cell stack with intermediate plates.

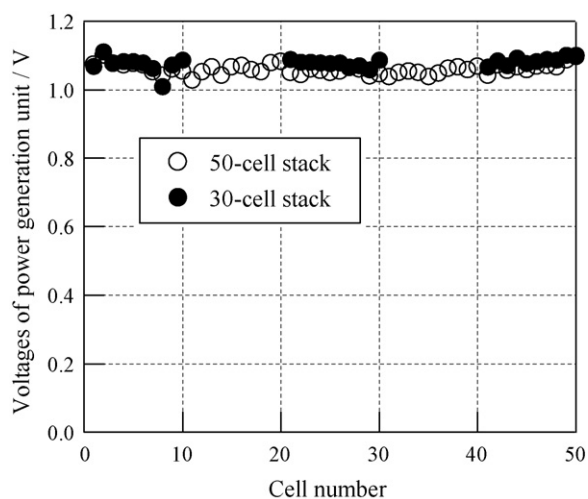


Fig. 6. Open circuit voltage of each power generation unit in 50- and 30-cell stacks with intermediate plates. Fuel flow rate: 10.5 L min^{-1} for 50-cell stack, 6.3 L min^{-1} for 30-cell stack. Air flow rate: 100 L min^{-1} for 50-cell stack, 60 L min^{-1} for 30-cell stack.

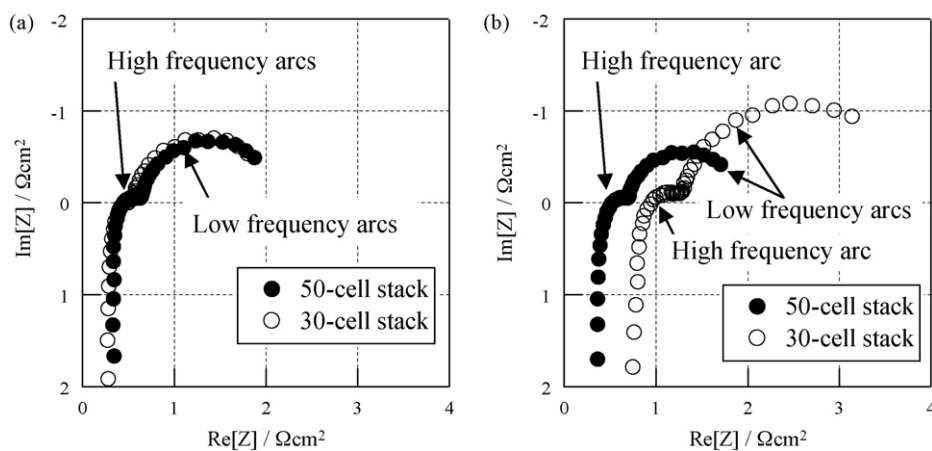


Fig. 7. Cole–Cole plots of AC impedance spectra of power generation units in 50- and 30-cell stacks with intermediate plates (a: power generation unit 1, b: power generation unit 21).

relative errors related to the position and angle of the stack parts and ensuring that they were arranged properly, thus stabilizing the stack condition and performance [12].

We disassembled the 50-cell stack with intermediate plates by separating the intermediate plates after 1200 h of operation. The intermediate plates exhibited hardly any deformation when compared with the metal plates composing the power generation units, since the former were thicker than the latter. Furthermore, the separated surfaces of the intermediate plates exhibited metallic luster. After the separation, we constructed a 30-cell stack with intermediate plates by piling up 10-cell sub-stacks as shown in Fig. 4.

The open circuit voltage (OCV) of each power generation unit in the 50- and 30-cell stacks with intermediate plates is shown in Fig. 6. Here, the OCV for the 50-cell stack was that after 1200 h of operation. For the 50- and 30-cell stacks, respectively, the fuel flow rates were 10.5 L min^{-1} and 6.3 L min^{-1} , and the air flow rates were 100 L min^{-1} and 60 L min^{-1} . At these fuel and air flow rates, the fuel and oxygen utilization was 60% and 15%, respectively, when the current density was 0.3 A cm^{-2} . The surface temperatures of the power generation units were $1078 \pm 5 \text{ K}$ also in the 30-cell stack. The OCV in the power generation unit 8 decreased to 1.01 V from 1.04 V. We estimate that the gas sealant performance decreased in the power generation unit 8. By contrast, the other power generation units exhibited no degradation in terms of OCV.

The Cole–Cole plots of the AC impedance spectra for representative power generation units in both the 50- and 30-cell stacks are shown in Fig. 7. There were little changes between the 50- and 30-cell stacks in the AC impedance spectra for all the power generation units except for the power generation unit 21. For example, the Cole–Cole plots of the AC impedance spectra for the power generation unit 1 in the 50- and 30-cell stacks were almost the same as shown in Fig. 7a. By contrast, the direct current resistance increased by 1.8 times (from $0.5 \Omega \text{ cm}^2$ to $0.9 \Omega \text{ cm}^2$) and both the low and high frequency arcs became larger in the power generation unit 21 as shown in Fig. 7b. For this power generation unit, we found that a transformed Cole–Cole plot of the AC impedance spectrum in the 30-cell stack, which is obtained by assuming that the active electrode area decreased by 0.56 ($=1/1.8$) times, was in good agreement with the original Cole–Cole plot in the 50-cell stack. It is suggested that the active electrode area decreased by 0.56 times in the power generation unit 21. We estimate that the contact between the cell and the separator became worse mainly at the cathode side, because the contact hardly becomes worse at the anode side since a deformable porous metal is placed there [11].

The relationships between the average unit voltage and the current density for the 50- and 30-cell stacks with intermediate plates

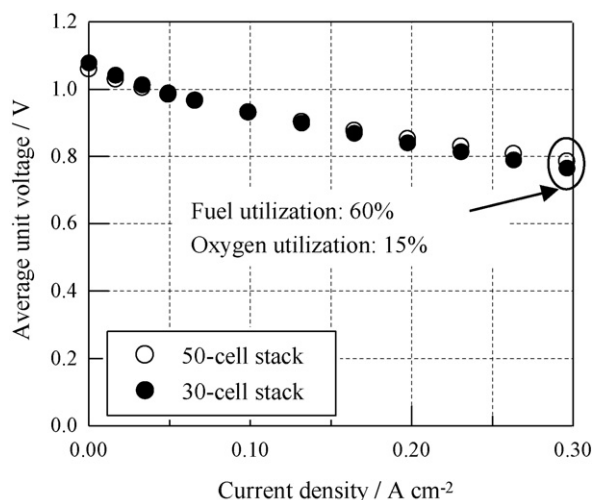


Fig. 8. Relationships between average unit voltage and current density for 50- and 30-cell stacks with intermediate plates.

are shown in Fig. 8. Here, the relationship for the 50-cell stack is that after 1200 h of operation. The hydrogen and air flow rates were determined so that the fuel and oxygen utilization were 60% and 15%, respectively, when the current density was 0.3 A cm^{-2} . Note that the voltage drop between the intermediate plates was considered at the average unit voltage since it was calculated by dividing the stack voltage by the number of power generation units. No significant loss in the stack performance was observed in the 30-cell stack. The degradation rate of the average unit voltages Δ was less than 3% at a current density of 0.30 A cm^{-2} . Here, the Δ value was calculated with the following equation:

$$\Delta = \frac{\bar{V}_{50} - \bar{V}_{30}}{\bar{V}_{50}} \times 100, \quad (1)$$

where \bar{V}_{50} and \bar{V}_{30} are average unit voltages of the 50- and 30-cell stacks, respectively. The surface temperatures of the power generation units were again $1083 \pm 5 \text{ K}$ at the current density of 0.3 A cm^{-2} in the 30-cell stack. The separation and reconnection of the 10-cell sub-stacks caused almost no degradation in terms of average unit voltage.

Fig. 9 shows the individual voltages of the power generation units in the 50- and 30-cell stacks with intermediate plates at a

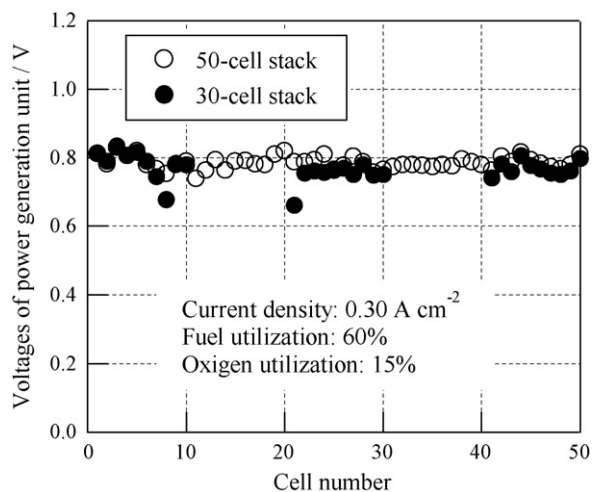


Fig. 9. Individual voltages of power generation units in 50- and 30-cell stacks with intermediate plates at current density of 0.3 A cm^{-2} .

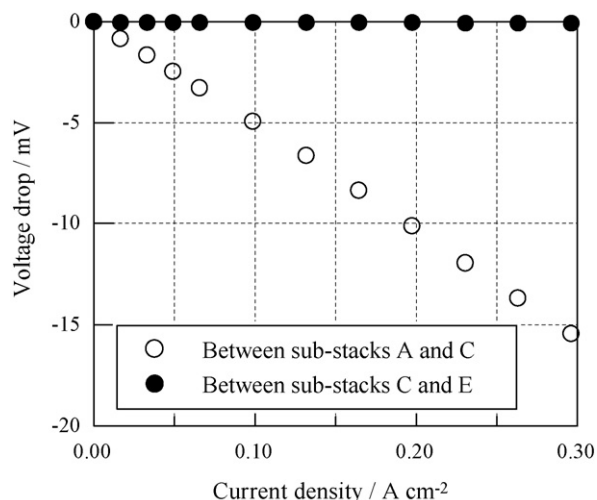


Fig. 10. Voltage drops between 10-cell sub-stacks in 30-cell stack with intermediate plates as a function of current density.

current density of 0.30 A cm^{-2} . The fuel and oxygen utilization was 60% and 15%, respectively. We calculated the degradation rate of each power generation unit δ^i as follows:

$$\delta^i = \frac{V_{50}^i - V_{30}^i}{V_{50}^i} \times 100, \quad (2)$$

where V_{50}^i and V_{30}^i are voltages of power generation units i in the 50- and 30-cell stacks, respectively. The δ^i value was no greater than 6% except for the power generation units 8 and 21, which exhibited large degradation rates of 10% and 16%, respectively. We estimate that the degradation in the power generation unit 8 had relation with the decrement of the OCV. Moreover, we consider that the changes in the AC impedance spectra explain the degradation in the power generation unit 21.

We measured the voltage drop between the 10-cell sub-stacks as shown in Fig. 4 as a function of current density and the result is shown in Fig. 10. There was almost no voltage drop observed between the 10-cell sub-stacks C and E. By contrast, a voltage drop, which was almost directly proportional to the current density, was observed between the 10-cell sub-stacks A and C. We consider that the contact condition was worse for the intermediate plates between the 10-cell sub-stacks A and C than between the 10-cell sub-stacks C and E. We estimated that the deformations of the

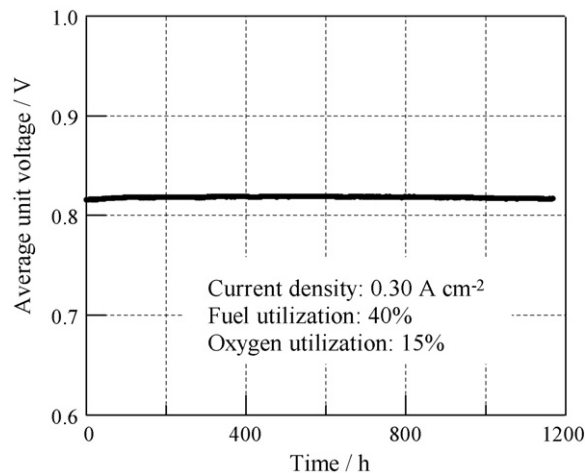


Fig. 11. Temporal change in average unit voltage for 30-cell stack with intermediate plates.

former intermediate plates were larger than those of the later intermediate plates. This problem should be dealt with in the future.

The temporal change in the average unit voltage for the 30-cell stack with intermediate plates is shown in Fig. 11. The current density, fuel utilization, and oxygen utilization were kept at 0.30 A cm^{-2} , 40%, and 15%, respectively. We tried to operate the 30-cell stack at a fuel utilization of 70% as well as we did with the 50-cell stack, but the fuel supply from the evaluation system became unstable because the absolute fuel flow rate decreased. Therefore we decided to operate the long-term test with a low fuel utilization of 40%. The 30-cell stack operated stably for about 1200 h. The average unit voltage increased by 0.3% for approximately the first 600 h, and it then decreased by 0.3% for roughly the last 600 h. It was shown that the stack provided acceptable durability after the separation and reconnection of the 10-cell sub-stacks. Here, it is also worth noting that the total power generation time for the cells in the 30-cell stack was about 2400 h (about 1200 h in the 50-cell stack and about 1200 h in the 30-cell stack).

We showed that the separation and reconnection of the 10-cell sub-stacks caused no significant loss of stack performance, which indicates that our stack can be restored by removing the 10-cell sub-stacks with broken cells and replacing them with undamaged 10-cell sub-stacks.

5. Conclusion

We investigated the influence of the separation and reconnection of the intermediate plates after high temperature operation in an SOFC stack equipped with two such plates every 10 power generation units. We showed that this separation and reconnection

caused no significant loss of stack performance. A 30-cell stack, which was constructed by removing two 10-cell sub-stacks from a 50-cell stack that had operated stably for 1200 h, functioned well. The difference between the average unit voltages of the 50- and 30-cell stacks was about 3% when the current density, fuel utilization, and oxygen utilization was 0.30 A cm^{-2} , 60%, and 15%, respectively. The 30-cell stack operated stably for about 1200 h. These findings indicate that our stack can be restored after some cells in the stack have broken down by removing the 10-cell sub-stacks that contain the broken cells and replacing them with undamaged 10-cell sub-stacks.

References

- [1] T. Ujiiie, ECS Transactions, 7 (2007) 3–9.
- [2] W.A. Surdoyal, ECS Transactions, 7 (2007) 11–15.
- [3] B. Rietveld, ECS Transactions, 7 (2007) 17–23.
- [4] H. Orui, K. Watanabe, R. Chiba, M. Arakawa, Journal of Electrochemical Society 151 (2004) A1412–A1427.
- [5] H. Orui, K. Nozawa, K. Watanabe, S. Sugita, R. Chiba, T. Komatsu, H. Arai, M. Arakawa, Journal of Electrochemical Society 155 (2008) B1110.
- [6] R. Chiba, F. Yoshimura, Y. Sakurai, Solid State Ionics 124 (1999) 281–288.
- [7] T. Komatsu, H. Arai, R. Chiba, K. Nozawa, M. Arakawa, K. Sato, Electrochemical and Solid State Letters 9 (2006) A9–A12.
- [8] T. Komatsu, H. Arai, R. Chiba, K. Nozawa, M. Arakawa, K. Sato, Journal of Electrochemical Society 154 (2007) B379–B382.
- [9] R. Chiba, H. Orui, T. Komatsu, Y. Tabata, K. Nozawa, H. Arai, M. Arakawa, K. Sato, ECS Transactions, 7 (2007) 1191–1200.
- [10] Y. Tabata, M. Yokoo, Y. Yoshida, K. Hayashi, K. Nozawa, Y. Nozaki, H. Arai, Proceedings of 2007 Fuel Cell Seminar and Exposition, 2007, p. 222.
- [11] M. Yokoo, Y. Tabata, Y. Yoshida, K. Hayashi, K. Nozawa, Y. Nozaki, H. Arai, Journal of Power Sources, 178/1 (2008) 59–63.
- [12] M. Yokoo, Y. Tabata, Y. Yoshida, H. Orui, K. Hayashi, Y. Nozaki, K. Nozawa, H. Arai, Journal of Power Sources 184 (2008) 84–89.